Confinement effects in PbSe quantum wells and nanocrystals

G. Allan* and C. Delerue
Institut d'Electronique, de Microélectronique et de Nanotechnologie (UMR CNRS 8520), Département ISEN, 41 boulevard Vauban, F-59046 Lille Cedex, France
(Received 15 March 2004; published 27 December 2004)

The effect of quantum confinement in PbSe quantum wells and dots is studied using tight binding calculations. Compared to zinc-blende semiconductors, unusual physical properties are predicted for rock salt PbSe nanostructures. The energy gap increases as the inverse of the size both for wells and dots. For PbSe nanocrystals, the luminescence lifetime, the confinement energy, and the intraband optical properties are in good agreement with experiments. The high quantum yield observed experimentally can be explained by the absence of surface dangling bonds in these systems. The origin of the second peak measured in the absorption spectra is discussed, whereas S-P interband transitions exhibit very small oscillator strength. The full frequency-dependent dielectric function $\epsilon(\omega)$ is calculated for PbSe quantum wells. Its imaginary part $\epsilon_2(\omega)$ is strongly anisotropic and shows large variations with respect to its bulk value even far from the gap region.

DOI: 10.1103/PhysRevB.70.245321 PACS number(s): 73.22.Dj, 78.67.Hc

I. INTRODUCTION

The effect of quantum confinement in semiconductor nanostructures has been intensively studied for more than two decades. On the experimental side, whereas most of the works have concerned III-V and II-VI semiconductors with zinc-blende or wurtzite structure, IV-VI semiconductors with cubic rock salt structure presently receive increasing attention due to their peculiar properties. In particular, PbSe, with its narrow gap ($\approx$280 meV at 300 K[1]) at the L point of the Brillouin zone and its large dielectric constant ($\epsilon_\infty \approx 23$), is a very promising material for opto-electronic applications. Owing to its small electron and hole effective masses ($<0.1\ m_0$[1,2]), the gap of confined PbSe structures can be tuned with size from its bulk value to about 2.0 eV.[3–15] The large exciton Bohr radius (46 nm) offers the possibility to study the strong confinement regime in relatively large structures.[16] Interesting optical properties have been observed in PbSe quantum wells made by molecular-beam epitaxy[15] and in nanocrystals, either electrodeposited on gold surfaces,[17] formed in an oxide glass host,[3–7] or obtained by colloidal chemistry in liquid solutions.[9–13] In the latter case, band-edge fluorescence is observed with a very high efficiency but with a long lifetime.[10,11] Infrared stimulated emission and optical gain have been reported in quantum-well-based devices[18–20] and in PbSe nanocrystals/sol-gel nanocomposites.[21] Intraband transitions have been also characterized by optically induced absorption.[10] Recent works have shown that the quantum confinement has also an important influence on the dielectric function far from the bandgap region,[17] in the visible and UV spectra.

On the theoretical side, PbSe nanostructures have been studied mainly using the envelope-function approximation and $\mathbf{k}\cdot\mathbf{p}$ Hamiltonians.[22–24] These approaches are very convenient to describe the physics of quantum confinement, but it is well-known that they may not be sufficiently accurate when the confinement energy becomes of the order of a few hundred of meV.[25,26] In addition, the optical properties of PbSe nanocrystals are not fully understood, and the predictions of $\mathbf{k}\cdot\mathbf{p}$ calculations have been questioned.[10,11] Indeed, the origin of the second peak in their absorption spectrum remains unclear: it is assigned either to the $1P_h$-$1S_e$ and $1S_h$-$1P_e$ transitions that are, in principle, parity forbidden,[8,11] or to transitions toward states resulting from the anisotropy of the band structure.[23] In addition, an inherent limitation of the envelope-function approximation is that it describes the electronic states only near the gap, and it does not allow one to calculate the full frequency-dependent dielectric function.

Thus, our aim in this paper is to study theoretically the electronic structure and the optical properties of PbSe nanostructures in a wide spectral range, from the infrared to the UV, which requires describing the full band structure of the material. Therefore, because *ab initio* methods are presently limited to small systems ($\lesssim$200 atoms), we present tight binding calculations[25,26] that allow us to address these problems for structures with sizes accessible to experiments. In the case of PbSe nanocrystals, we compare our results to those obtained previously on the basis of a $\mathbf{k}\cdot\mathbf{p}$ Hamiltonian. We show that tight binding calculations predict confinement energies, fluorescence lifetimes and intraband optical properties in good agreement with experiments and we discuss the issue related to forbidden transitions in the absorption spectrum. In the case of PbSe quantum wells, we show that the confinement has profound and unusual effects on the optical transitions involving electronic states which are deep in the bands, i.e., far from the gap region.[17]

The paper is organized as follows. In the next section, we describe the tight binding method and the formalism used to calculate the optical matrix elements. We discuss the electronic structure and the optical properties of bulk PbSe to validate the method and to emphasize some unusual properties of the material. In Sec. III, we consider PbSe quantum wells. We present the evolution of the complex dielectric constant as a function of the width of the wells, and we study the anisotropy of the optical response. Section IV is devoted to the interband and intraband transitions in PbSe nanocrystals. We conclude the paper in Sec. V.

TABLE I. Top: first nearest neighbor tight binding parameters for PbSe. The notation is that of Slater and Koster (Ref. 27) (a = anion, c = cation). Δ is the spin-orbit coupling parameter. Bottom: longitudinal (l) and transverse (t) effective masses for the conduction (e) and valence (h) bands at the L point in units of the free-electron mass.

Tight binding parameters for PbSe	
Intra-atomic terms:	
$E_s^a = -11.45405$ eV	$E_s^c = -5.07781$ eV
$E_p^a = -1.47533$ eV	$E_p^c = 4.33168$ eV
$E_d^a = 12.13125$ eV	$E_d^c = 10.97439$ eV
$E_{s^*}^a = 17.60374$ eV	$E_{s^*}^c = 24.35922$eV
$\Delta^a = 0.24000$ eV	$\Delta^c = 0.55000$ eV
First nearest neighbor interactions:	
$E_{ss\sigma}$(ac) $= -0.36267$ eV	
$E_{s^*s^*\sigma}$(ac) $= -0.93835$ eV	
$E_{ss^*\sigma}$(ac) $= -1.12089$ eV	$E_{ss^*\sigma}$(ca) $= -1.29525$ eV
$E_{sp\sigma}$(ac) $= 1.20593$ eV	$E_{sp\sigma}$(ca) $= 1.31029$ eV
$E_{s^*p\sigma}$(ac) $= 2.51117$ eV	$E_{s^*p\sigma}$(ca) $= 2.27510$ eV
$E_{sd\sigma}$(ac) $= -0.83693$ eV	$E_{sd\sigma}$(ca) $= -1.71725$ eV
$E_{s^*d\sigma}$(ac) $= -0.92754$ eV	$E_{s^*d\sigma}$(ca) $= 0.18794$ eV
$E_{pp\sigma}$(ac) $= 1.71542$ eV	$E_{pp\pi}$(ac) $= -0.38235$ eV
$E_{pd\sigma}$(ac) $= -1.07458$ eV	$E_{pd\sigma}$(ca) $= -2.13886$ eV
$E_{pd\pi}$(ac) $= -0.14844$ eV	$E_{pd\pi}$(ca) $= 0.73701$ eV
$E_{dd\sigma}$(ac) $= -0.27384$ eV	$E_{dd\pi}$(ac) $= 1.48923$ eV
$E_{dd\delta}$(ac) $= -0.35624$ eV	
Effective masses:	
$m_t^e = 0.0462$	$m_t^h = 0.0472$
$m_l^e = 0.0374$	$m_l^h = 0.0468$

II. BULK SEMICONDUCTOR

A. Tight binding calculations

The electronic structure of PbSe is calculated in tight binding, following the method described in Ref. 25. The Hamiltonian matrix is written in a $sp^3d^5s^*$ basis, the overlaps are neglected, and the hopping integrals are restricted to first nearest neighbor interactions. Because Pb is a heavy element, we include the spin-orbit coupling which requires doubling the basis set. The parameters (Table I) are obtained by fitting the experimental effective masses and a reference band structure at the main points of the Brillouin zone and in a large energy range. This reference band structure was calculated using the *ab initio* pseudopotential code ABINIT[28,29] in the local density approximation. The band structure obtained in tight binding [Fig. 1(a)] is in good agreement with those previously reported in the literature.[30–34] We obtain an energy gap E_g of 0.176 eV, but it is important to point out that experimentally the energy gap of bulk PbSe is strongly dependent on the temperature ($E_g = 125 + \sqrt{400 + 0.256T^2}$ meV),[1,33] and that in quantum dots this temperature variation is size dependent.[5]

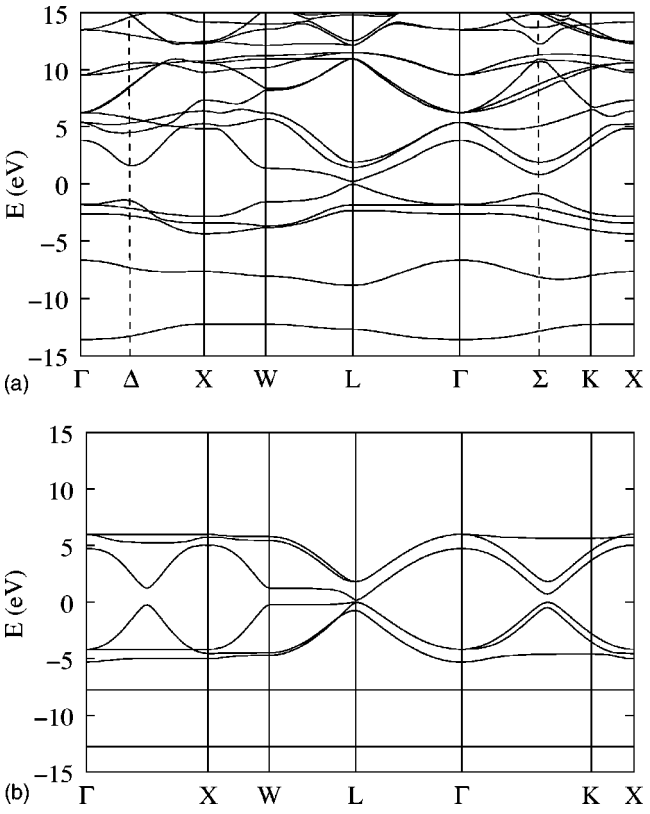

FIG. 1. (a) Band structure of bulk PbSe. The zero of energy corresponds to the top of the valence band. (b) Same but with $E_{pp\sigma}$(ac) = 2.5 eV, $E_p^c - E_p^a = 1.5$ eV and the spin-orbit coupling keeping its bulk value, all other interatomic terms of the Hamiltonian being set to zero.

In the case of quantum wells and dots, the tight binding parameters are transferred without change from the bulk situation using the appropriate boundary conditions. Since PbSe is a strongly ionic material, we do not passivate the surfaces as in the case of III-V semiconductor nanocrystals for which pseudo-hydrogen atoms are required to saturate the dangling bonds and to push the surface states far from the energy gap.[25] We will discuss the consequences of this assumption and the influence of surfaces later. To account for the electronic relaxation near the surfaces, we apply an intra-atomic potential of −0.18 eV on each surface atom to achieve charge neutrality.[35]

B. Complex dielectric function

Once the electronic structure is obtained, we calculate the complex frequency-dependent dielectric function $\epsilon(\omega) = \epsilon_1(\omega) + i\epsilon_2(\omega)$. In the case of interband transitions, its imaginary part $\epsilon_2(\omega)$ is given by

$$\epsilon_2(\omega) = \frac{4\pi^2 e^2}{m_0^2 \omega^2 \Omega} \sum_{i,j} \delta(E_{c,i} - E_{v,j} - \hbar\omega) \times |\langle u_{c,i}|\mathbf{e}\cdot\mathbf{p}|u_{v,j}\rangle|^2, \tag{1}$$

where $u_{c,i}$ and $u_{v,j}$ are the conduction and valence wave functions of energy $E_{c,i}$ and $E_{v,j}$, respectively. Ω is the volume of

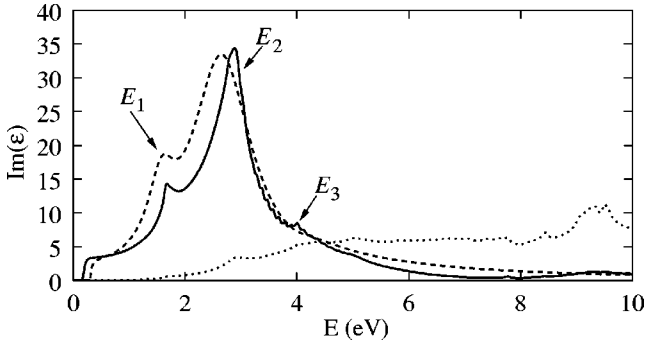

FIG. 2. Imaginary part of the frequency-dependent dielectric function $\epsilon_2(\omega)$ for bulk PbSe calculated in tight binding (solid line) compared to the experimental value at 300 K of Ref. 40 (dashed line) and to the calculated joint density of states (dotted line). E_1, E_2, and E_3 indicate the main transitions at critical points of the band structure.

the system, and **e** is the polarization vector of the light. For bulk PbSe, the wave functions and the energies are obtained by diagonalizing the Hamiltonian at $\approx 8\times 10^6$ points in the the Brillouin zone.

The matrix elements of **p** are calculated following Refs. 36–38. To this end, let us consider atomic orbitals $|\alpha,\mathbf{R}\rangle$ centered at position **R** and characterized by a label α. We write

$$\langle \alpha,\mathbf{R}|\mathbf{p}|\beta,\mathbf{R}'\rangle = \frac{m_0}{i\hbar}\Big\{(\mathbf{R}-\mathbf{R}')\langle \alpha,\mathbf{R}|H|\beta,\mathbf{R}'\rangle + \sum_{\gamma}\left[\langle \gamma,\mathbf{R}|H|\beta,\mathbf{R}'\rangle d_{\alpha\gamma} - \langle \alpha,\mathbf{R}|H|\gamma,\mathbf{R}'\rangle d_{\gamma\beta}\right]\Big\}, \tag{2}$$

where the terms $d_{\alpha\gamma}=\langle \alpha,\mathbf{R}|\mathbf{r}|\gamma,\mathbf{R}\rangle$ describe intra-atomic polarizations. The simplest approximation involves setting all these intra-atomic terms to zero since there are no adjustable parameters beyond those for the Hamiltonian.[37] However, we have chosen to use Eq. (2) with intra-atomic terms calculated from free-atom orbitals:[39] we checked that it gives results in good agreement with experiments in many situations (see also Ref. 38). This is confirmed by Fig. 2, in which we compare our predictions for the imaginary part of the dielectric function for bulk PbSe to measurements of Ref. 40.

The main features of $\epsilon_2(\omega)$ (Fig. 2) occur at van Hove singularities in the joint density of states,[30] at the L point and on the axes Σ and Δ of the Brillouin zone (see Fig. 1). Following the notations of Ref. 41, the threshold E_0 coincides with the energy gap at the L point and corresponds to the transition $L_{5\to 6}$ (with the usual notation,[30] 1 is the deepest band of Fig. 1). The shoulder E_1 at $\approx$1.7 eV corresponds mainly to $\Sigma_{5\to 6}$, and the main peak E_2 at $\approx$2.8 eV to $\Delta_{5\to 6}$ and $\Sigma_{5\to 7}$. Finally, the third peak E_3 at $\approx$4.1 eV takes place at $\Delta_{4\to 6}$ and $\Sigma_{4\to 7}$.

III. QUANTUM WELLS

In this section, we consider PbSe quantum wells with (001) surfaces. We discuss the existence of surface states,

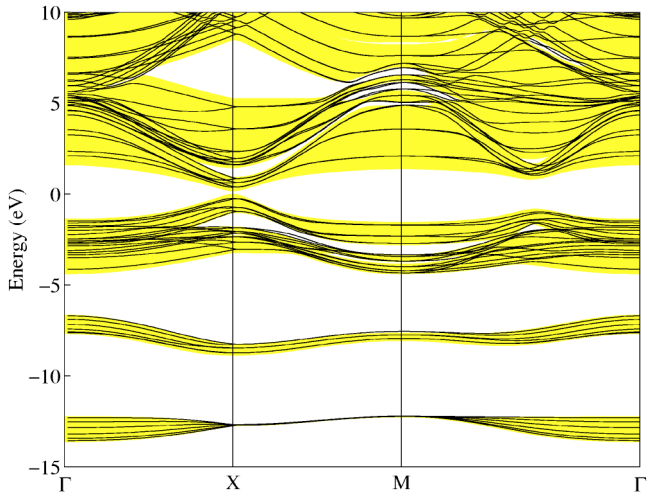

FIG. 3. Lines: band structure of a well containing six PbSe planes. Shaded region: projection of the bulk band structure on the surface reciprocal space.

and next the effect of the confinement, first on the energy gap, second on the frequency-dependent dielectric function.

Figure 3 compares the band structure of a PbSe well with a projection of the bulk band structure in the two-dimensional k-space. It shows that surfaces do not introduce states in the energy gaps of the bulk band structure, even though they are not passivated. This is due to the fact that the electronic states are mainly p-like (evidence will be given later). In a finite system of atoms characterized by p orbitals, even the p orbitals at surfaces remain strongly coupled with orbitals of atoms at the interior. This is in contrast with zinc-blende semiconductors described by hybrid sp^3 orbitals which, to a first approximation, remain uncoupled at surfaces, forming dangling bonds.[42] The absence of dangling bonds at surfaces could explain the high fluorescence efficiency of PbSe nanostructures[10,11] in spite of a long lifetime, and also the small Stokes shift between emission and absorption.[10,11,21]

A. Energy gap

Figure 4 shows the evolution with size of the confinement energy (i.e., the increase in the energy gap) in quantum wells. Disregarding the small difference between wells with odd and even numbers of PbSe planes, the average energy gap (in eV) is given by

$$E_g(L) = E_g(\infty) + \frac{1}{1.2125L + 0.3326}, \tag{3}$$

where L is the well thickness in nanometer ($L=Na/2$, where N is the number of planes and a is the lattice parameter). The $1/L$ dependence of the energy gap is quite unusual, since simple effective mass theory predicts a $1/L^2$ law.[42] The reason is that the energy dispersion is mostly linear around the gap (see Fig. 1) and is parabolic only in a very small region near the extrema (Fig. 5). This result shows that the effective masses are not pertinent quantities to predict the effect of the quantum confinement in PbSe nanostructures.

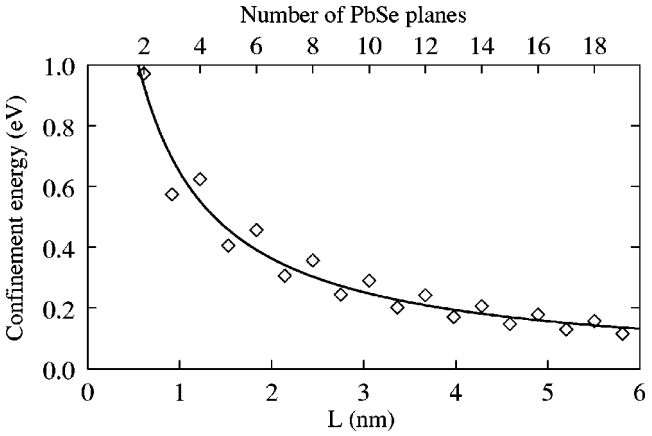

FIG. 4. Squares confinement energy in quantum wells as a function of size. Line: fit of the energy gap.

B. Dielectric function

Figure 6 presents the evolution of the imaginary part of the frequency-dependent dielectric function with respect to the well thickness. Two polarizations are considered: **e** along [100] and [001]. For thin wells, $\epsilon_2(\omega)$ becomes strongly anisotropic. For in-plane polarization ($\mathbf{e}\|[100]$), $\epsilon_{2\|}(\omega)$ remains all the time close to the bulk value, with anyway some differences that we will discuss later. On the contrary, with a polarization perpendicular to the surfaces ($\mathbf{e}\|[001]$), the dielectric function $\epsilon_{2\perp}(\omega)$ has a huge dependence on size. This unusual behavior is due to the peculiar electronic structure of PbSe, and more generally of lead-salt semiconductors. To understand this, we show in Fig. 1(b) the band structure of bulk PbSe when all the tight binding interaction parameters are switched to zero, except the spin-orbit coupling and the hopping integral $pp\sigma$. The resulting band structure [Fig. 1(b)] is remarkably close to the true one [Fig. 1(a)], which means that, when considering its electronic properties, bulk PbSe is basically equivalent to a set of independent chains of p orbitals along the x, y, and z axes (Fig. 7). Thus, in wells with (001) surfaces, the chains of p_z orbitals are finite and their electronic structure depends strongly on size, according

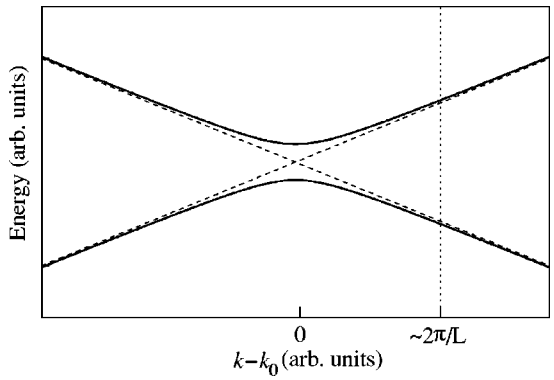

FIG. 5. The energy dispersion in bulk PbSe is mostly linear except very close to the gap region, where it becomes parabolic. The confinement energy behaves as $1/L$, where L is the size of the nanostructure. k_0 is the wave vector at the L point ofthe Brillouin zone.

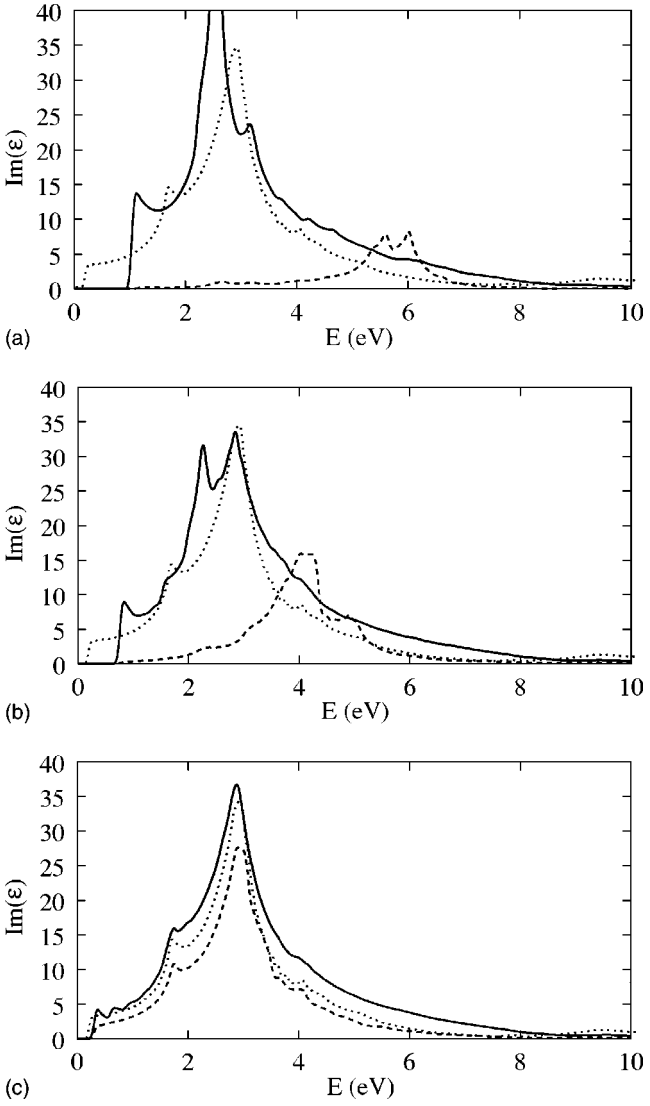

FIG. 6. Imaginary part of the frequency-dependent dielectric function $\epsilon_2(\omega)$ of quantum wells made of 2 (a), 4 (b), and 20 (c) PbSe (001) planes. The solid lines are for a polarization vector e parallel to the planes $\{\epsilon_{2\|}(\omega)$, along [100]$\}$ and the dashed lines for **e** perpendicular $\{\epsilon_{2\perp}(\omega)$, along [001]$\}$. The dotted lines represent $\epsilon_2(\omega)$ calculated for bulk PbSe.

to usual quantum confinement effects. On the contrary, chains of p_x and p_y orbitals remain infinite, as in the bulk material. Thus, the anisotropy comes from the fact that $\epsilon_{2\perp}(\omega)$ arises from the polarization of the bonds along the chains of p_z orbitals, whereas $\epsilon_{2\|}(\omega)$ comes from the in-plane polarization, which is bulk-like.

Obviously, the previous picture is too simplified, and there are weak couplings between the chains (e.g., through the spin-orbit coupling or via the s orbitals). As a consequence, confinement effects are also visible in $\epsilon_{2\|}(\omega)$. Let us consider, for example, the well made of four PbSe planes [Fig. 6(b)]. The optical threshold is blueshifted, following the usual confinement effect at the energy gap, here at the L point. The situation at higher energy is much more unusual,[17] and is once again the consequence of the peculiar electronic structure of PbSe. The peaks E_1, E_2, and E_3 are still present,

FIG. 7. The electronic structure of bulk PbSe can be described by linear chains of p orbitals with only $pp\sigma$ interactions.

at almost the same energy as in the bulk. However, there are additional peaks, in particular at ≈2.5 and ≈3.5 eV. To understand this behavior, we must study the effect of the confinement at the critical points of the Brillouin zone, where there are van Hove singularities in the bulk case. For example, E_1 arises mainly from the transitions $\Sigma_{5\to6}$. However, the critical points along Σ are saddle points for bands 5 and 6, and therefore the effect of the confinement depends on the orientation of the Σ axis with respect to the growth axis [001]. If there is a local minimum of the energy gap along [110] when plotted in this direction [Fig. 1(a)], Fig. 8 shows that it is a maximum when plotted in the [001] direction. Thus, the confinement in the [001] direction gives rise to a redshift for critical points along [110], $[\bar{1}10]$, $[1\bar{1}0]$, and $[\bar{1}\bar{1}0]$ axes, and a blueshift for the others (e.g., [101], [011],…). Thus, the peak at ≈2.5 eV arises from the blueshifted $\Sigma_{5\to6}$ transitions.[43] For the redshifted ones, the shift is actually very small, nearly imperceptible, because the bands are almost flat in the [001] direction as shown in Fig. 8 (it is completely flat when the coupling between chains is neglected). This explains the presence of a peak near E_1, almost as in bulk PbSe.

The same analysis can be performed for $\Sigma_{5\to7}$ and for $\Delta_{5\to6}$, explaining the peaks at E_2 and their counterparts, which are blueshifted near 3.5 eV. Note that the critical points along Δ ([100] directions) are also saddle points for bands 5 and 6: the local minimum of the energy gap along [100] is a maximum along [001].

IV. NANOCRYSTALS

Figure 9 presents the confinement energy in PbSe nanocrystals as function of size. Interestingly, very close results are obtained for cubic and spherical dots with the same volume, as already obtained for other semiconductors.[26,44] The energy gap (in eV) is given by

$$E_g(D) = E_g(\infty) + \frac{1}{0.0105D^2 + 0.2655D + 0.0667}, \quad (4)$$

where D is the effective diameter of the dot in nanometer (for a cube, the diameter of the sphere with the same volume). As in the case of quantum wells, the energy gap varies mainly as $1/D$ (the coefficient of D^2 is small), and there is no surface state in the gap. Our predicted gaps are in good agreement with experiments (Fig. 9), taking into account the dispersion of measured values.

A. Interband transitions

We consider now the optical absorption in PbSe nanocrystals. Figure 10(a) presents results for dot sizes of ≈7 nm, i.e., containing ≈7000 atoms. For such large sizes, it is not possible to make a full diagonalization of the Hamiltonian matrix and we must use an efficient gradient conjugate method[26] to calculate the eigenstates only close to the gap. The decrease to zero of the absorption spectra above 1.2 eV is just a consequence of the limited number of eigenstates that we can calculate. Figure 10(a) compares a measured absorption spectrum[9] with those predicted for spherical and cubic nanocrystals characterized by the same volume. The lowest calculated peak corresponds to $1S_h-1S_e$ transitions. It includes 64 lines resulting from the eightfold degeneracy of the extrema at the L point of the Brillouin zone. The second and third calculated peaks arise from $1P_h-1P_e$ and $1D_h-1D_e$ transitions. These three peaks agree well with structures in the experimental spectrum,[9] confirming previous interpretations.[11] However, the experimental peak at ≈0.8 eV is not reproduced by the calculations. In fact, we obtain that the energy of this peak fits well with $1S_h-1P_e$ and $1P_h-1S_e$ transitions, as shown by plotting the joint density of states [Fig. 10(b)],[45] but we find that S-P transitions are almost completely forbidden. The prediction made with a $\mathbf{k}\cdot\mathbf{p}$ Hamiltonian that the observed peak could result from anisotropy effects[23] is not supported by our calculation. In cubic nanocrystals, we calculate that the selection rules for S-P transitions are slightly relaxed, but the amplitude of the peak remains much smaller than the observed one [it is almost not visible in Fig. 10(a)]. We also performed calculations on nanocrystals with more complex shapes and with fewer symmetries, but we never found a second peak with the correct amplitude compared to experiments.

Thus, one important conclusion of our work is that direct S-P transitions are not allowed, and other physical effects must be studied to explain the relaxation of the selection

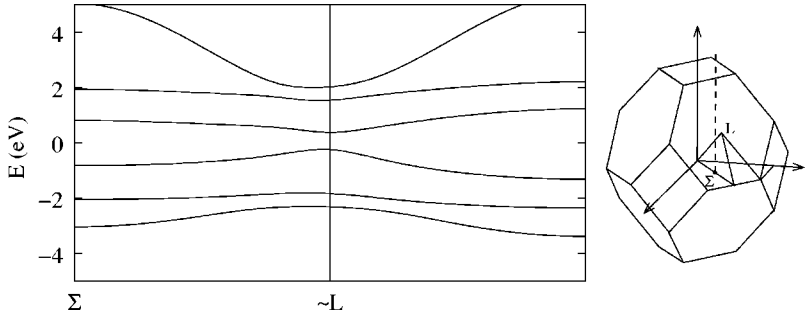

FIG. 8. Band structure of bulk PbSe in the [001] direction starting from the critical point Σ along the [110] axis (along the dashed line in the Brillouin zone).

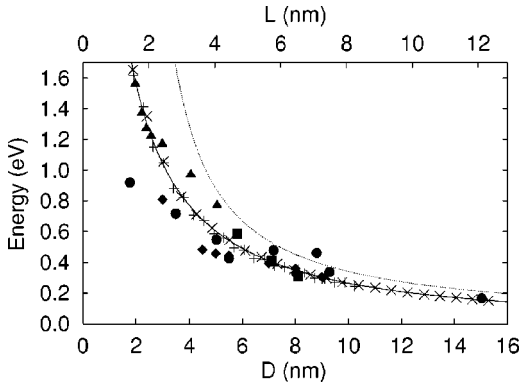

FIG. 9. Calculated confinement energy in spherical (×) and cubic (+) PbSe nanocrystals as function of size (diameter D for a sphere, side length L for a cube). Cubes and spheres with the same volume are at the same abscissa [$L=D(\pi/6)^{1/3}$]. Continuous line: fit of the results. Dotted line: $\mathbf{k}\cdot\mathbf{p}$ results of Ref. 3. Experimental values (first excitonic transition): Ref. 10 (■), Ref. 3 (●), Ref. 12 (▲), and Ref. 9 (♦).

rules. One possible explanation could be that S-P transitions become allowed via phonon-assisted processes. There are four equivalent extrema at the L point of the Brillouin zone, giving rise to S and P states in each valley, and transitions between these states could occur via intervalley scattering. We have recently calculated that similar processes are very efficient in the case of Si nanocrystals.[46] Permanent dipole moments in the nanocrystals are also proposed for breaking the selection rule.[47]

It is often assumed that the four equivalent extrema at the L point of the Brillouin zone together with a twofold spin degeneracy lead to a eightfold degeneracy of the quantized states.[9,21,22] Tight binding calculations confirm that the lowest conduction states and the highest valence states are grouped into well-defined multiplets of eight levels, but there are splittings between these levels due to intervalley couplings. These couplings are not described by $\mathbf{k}\cdot\mathbf{p}$ Hamiltonians, which assume independent valleys. Figure 11 shows that the splittings are substantial in a wide range of nanocrystal sizes (often larger than kT even at room temperature). It is important to notice that intervalley splittings are a decreasing function of size but with important oscillations,[26,48] explaining why the ordering of the states (and their degeneracy) seems to scatter from one dot to another.

Experiments show that PbSe nanocrystal colloids fluoresce efficiently[10,11] but with a long lifetime in the microsecond range.[10] To understand this behavior, we have calculated the radiative recombination lifetime τ_{ij} between conduction states $|u_{c,i}\rangle$ and valence states $|u_{v,j}\rangle$ in the dipolar approximation using[42]

$$\frac{1}{\tau_{ij}} = \frac{4\omega_{ij}^3 F^2 e^2 r_{ij}^2 n_{op}}{3c^3\hbar}, \tag{5}$$

with

$$r_{ij}^2 = |\langle u_{c,i}|x|u_{v,j}\rangle|^2 + |\langle u_{c,i}|y|u_{v,j}\rangle|^2 + |\langle u_{c,i}|z|u_{v,j}\rangle|^2. \tag{6}$$

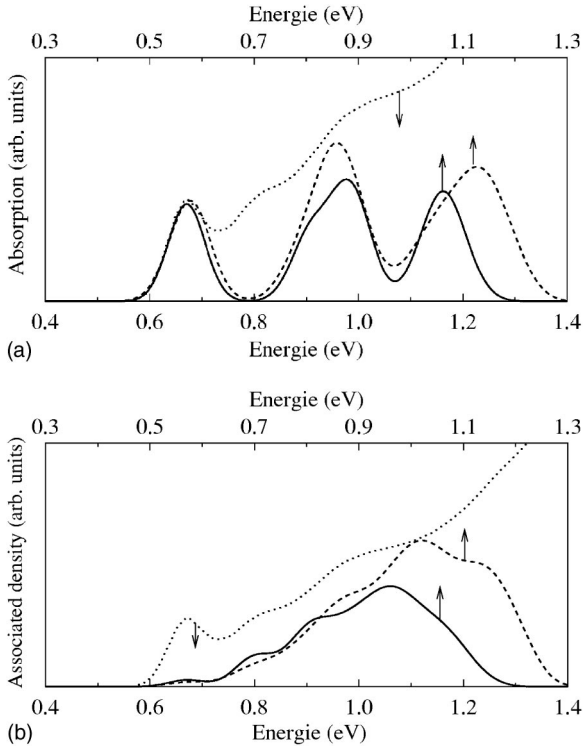

FIG. 10. (a) Optical absorption spectrum of PbSe nanocrystals, each transition line being broadened by a Gaussian (width =35 meV). Continuous line: theory, sphere (diameter=7.3 nm). Dashed line: theory, cube (side (length=7.2 nm). Dotted line: experiments of Ref. 9 (average (diameter=7 nm). (b) Same, but the theory shows the joint density of states; i.e., replacing the optical matrix element by a constant. Note that for the sake of comparison, the lower energy scale of the experimental spectrum is slightly shifted with respect to the upper one of theoretical spectra (shift =0.1 eV).

In Eq. (5), ω_{ij} is the transition frequency, F is the local field factor, and n_{op} is the macroscopic refractive index of the system. In the case of spherical dots of dielectric constant ϵ_{in} embedded in a medium of dielectric constant ϵ_{out}, we

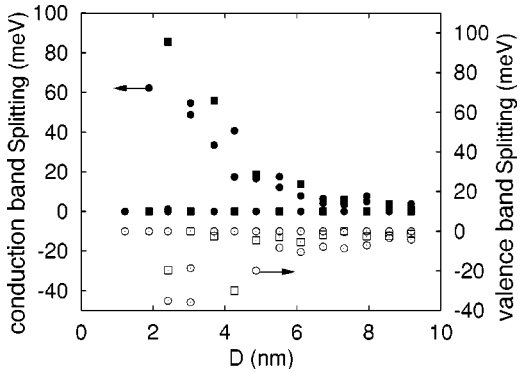

FIG. 11. Splittings of the energy levels in the conduction band (full symbols) and in the valence band (empty symbols) of spherical PbSe nanocrystals as a function of their diameter. The splittings are defined with respect to the lowest unoccupied level and to the highest occupied level, respectively. The levels have either a twofold (circle) or a fourfold (square) degeneracy.

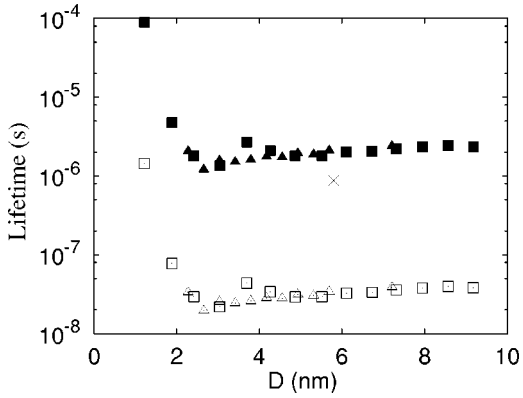

FIG. 12. Evolution with size of the radiative lifetime in spherical (□, ■) and cubic (△, ▲) nanocrystals. Empty symbols correspond to lifetimes calculated with $\epsilon_{in}=23$ and $\epsilon_{out}=23$, filled ones to those calculated with $\epsilon_{in}=23$ and $\epsilon_{out}=2.1$. The cross is the measured lifetime of Ref. 10.

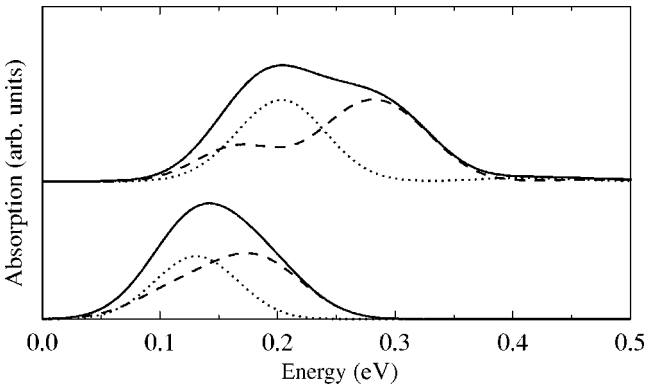

FIG. 13. Room temperature intraband optical absorption in the conduction (dotted line) and valence (dashed line) band of spherical nanocrystals charged with one extra electron or one extra hole, respectively (upper curves: diameter=4.9 nm; lower ones=7.3 nm). Continuous line: sum of electron and hole contributions.

have[10,42] $n_{op}\approx\sqrt{\epsilon_{out}}$ and $F\approx 3\epsilon_{out}/(\epsilon_{in}+2\epsilon_{out})$. We suppose that the local field factor F remains the same for cubic dots. Using the values of τ_{ij}, we calculate the average radiative lifetime of one electron-hole pair in a nanocrystal at a given temperature, assuming that the electron and the hole are in thermal equilibrium within the conduction and valence states, respectively. This approximation of quasi-equilibrium is justified by the fast relaxation of the carriers within their respective bands.[10] Results for the average lifetime are shown in Fig. 12. We consider two cases: a first one with $\epsilon_{in}=23$ and $\epsilon_{out}=23$, which could correspond to the limit of a packed array of nanocrystals, a second one with $\epsilon_{in}=23$ and $\epsilon_{out}=2.1$, simulating the experimental situation of Ref. 10 where colloids are dissolved in chloroform. Interestingly, cubic and spherical dots give similar lifetimes. In agreement with experiments, we confirm that there is no need to invoke a triplet transition to explain long lifetimes.[10] The small discrepancy between our results for $\epsilon_{out}=2.1$ and the experimental value of 0.88 μs[10] could be easily interpreted by a reduction of the average dielectric constant in the nanocrystals compared to its bulk value (=23), as discussed, for example, in Ref. 49, or by a slightly higher value of ϵ_{out}.

B. Intraband transitions

We consider now intraband transitions in which PbSe nanocrystals contain one extra electron, one extra hole, or an electron-hole pair. The induced absorption spectra corresponding to these situations are shown in Fig. 13. Replacing each transition line by a Gaussian (width=35 meV), we obtain that the spectra are very broad, due to the fact that the S and P levels arising from the four equivalent valleys and from the two directions of spin are split by anisotropy effects, spin-orbit, and intervalley couplings. We find that the broadening increases with decreasing size. Interestingly, broad spectra are observed experimentally,[10] with linewidths close to our predictions (obviously inhomogeneous broadening also plays a role). The induced absorption spectra calculated for an extra electron present one peak, whereas hole transitions give rise to two peaks for dot diameters below 6 nm (above, the lowest energy peak is no longer distinguishable). We plot in Fig. 14 the evolution with size of the peak maxima. The transition energies vary once again as $1/D$. We also show the experimental results of Ref. 10. The agreement with our values is good, taking into account that the spectra are broad and that experimental data obtained by optically induced absorption[10] correspond to excitations of both electrons and holes.

V. CONCLUSIONS

We presented a theoretical study of the electronic structure and of the optical properties of PbSe layers and nanocrystals. Under confinement, the energy gap varies as the inverse of the size, which comes from the almost linear energy dispersion of bulk bands. Because the electronic states are mostly *p*-like, the surfaces do not create localized states in the gap, which could explain the high fluorescence efficiency

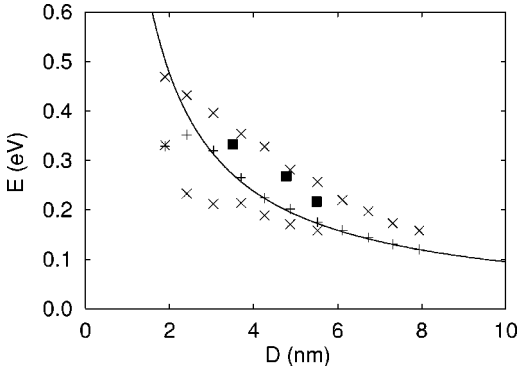

FIG. 14. Evolution with diameter D of the energy of the main intraband transitions in the conduction band (+) and in the valence band (×) of spherical nanocrystals compared to the experimental values (■) of Ref. 10, the size being deduced from the energy of the first exciton peak using Eq. (4). Straight line: fit of the electron intraband transition energy (E in eV, D in nanometer): $E=1/(1.05D)$.

of the nanostructures. This result naturally explains why, to our knowledge, no trapped states have been observed experimentally. We predict similar confinement energies in spherical and cubic nanocrystals. The calculated excitonic energies and radiative lifetimes of dots are in good agreement with experiments. However, one question remains: why the second observed exciton seems to be optically allowed, whereas we predict a vanishing oscillator strength. In nanocrystals, we show that the four equivalent extrema at the *L* point of the Brillouin zone do not lead to an eightfold degeneracy of the quantum states due to intervalley couplings. This could explain why the expected degeneracy is not apparent in the bleach data of Ref. 10. We predict that intraband transitions induced by an extra particle give rise to broad peaks, due to splittings between states originating from different valleys.

In the case of PbSe quantum wells, calculations show that the confinement leads to a strong anisotropy of the dielectric function. The main transitions at the critical points of the Brillouin zone are also influenced by the confinement, as shown by ellipsometry measurements on PbSe layers.[17] All these results demonstrate the originality of the optical properties in PbSe nanostructures.

ACKNOWLEDGMENTS

Work supported in part by the European Community's Human Potential Programme under Contract No. HPRN-CT-2002-00320, NANOSPECTRA.

*Electronic address: guy.allan@isen.iemn.univ-lille1.fr

[1] Landolt-Bornstein, *Semiconductors: Physics of Nontetrahedrally Bonded Binary Compounds II* (Springer-Verlag, Berlin, 1983), Vol. III/17f.
[2] A. Santoni, G. Paolucci, G. Santoro, K.C. Prince, and N.E. Christensen, J. Phys.: Condens. Matter **4**, 6759 (1992).
[3] A. Lipovskii, E. Kolobkova, V. Petrikov, I. Kang, A. Olkhovets, T. Krauss, M. Thomas, J. Silcox, F. Wise, Q. Shen, and S. Kycia, Appl. Phys. Lett. **71**, 3406 (1997).
[4] P.T. Guerreiro, S. Ten, N.F. Borelli, J. Butty, G.E. Jabbour, and N. Peyghambarian, Appl. Phys. Lett. **71**, 1595 (1997).
[5] A. Olkhovets, R.-C. Hsu, A. Lipovskii, and F.W. Wise, Phys. Rev. Lett. **81**, 3539 (1998).
[6] K. Wundke, S. Potting, J. Auxier, A. Schülzgen, N. Peyghambarian, and N.F. Borelli, Appl. Phys. Lett. **76**, 10 (2000).
[7] K. Wunkde, J. Auxier, A. Schülzgen, N. Peyghambarian, and N.F. Borelli, Appl. Phys. Lett. **75**, 3060 (1999).
[8] F.W. Wise, Acc. Chem. Res. **33**, 773 (2000).
[9] C.B. Murray, S. Sun, W. Gaschler, H. Doyle, T.A. Betley, and C.R. Kagan, IBM J. Res. Dev. **45**, 47 (2001).
[10] B.L. Wehrenberg, C. Wang, and P. Guyot-Sionnest, J. Phys. Chem. B **106**, 10634 (2002).
[11] H. Du, C. Chan, R. Krishnan, T.D. Krauss, J.M. Harbold, F.W. Wise, M.G. Thomas, and J. Silcox, Nano Lett. **2**, 1321 (2002).
[12] A. Sashchiuk, L. Langof, R. Chaim, and E. Lifshitz, J. Cryst. Growth **240**, 431 (2002).
[13] A. Sashchiuk, L. Amirav, M. Bashouti, M. Krueger, U. Sivan, and E. Lifshitz, Nano Lett. **4**, 159 (2004).
[14] Z. Hens, B. Grandidier, D. Deresmes, G. Allan, C. Delerue, D. Stiévenard, and D. Vanmaekelbergh, Europhys. Lett. **65**, 809 (2004).
[15] H. Wu, N. Dai, and P.J. McCann, Phys. Rev. B **66**, 045303 (2002).
[16] A.L. Efros and A.L. Efros, Sov. Phys. Semicond. **16**, 772 (1982).
[17] Z. Hens, D. Vanmaekelbergh, E.S. Kooij, H. Wormeester, G. Allan, and C. Delerue, Phys. Rev. Lett. **92**, 026808 (2004).
[18] Z. Shi, M. Tacke, A. Lambrecht, and H. Bottner, Appl. Phys. Lett. **66**, 2537 (1995).
[19] U.P. Schliessl and J. Rohr, Infrared Phys. Technol. **40**, 325 (1999).
[20] C.L. Felix, W.W. Bewley, I. Vurgaftman, J.R. Lindle, J.R. Meyer, H.Z. Wu, G. Xu, S. Khosravani, and Z. Shi, Appl. Phys. Lett. **78**, 3770 (2001).
[21] R.D. Schaller, M.A. Petruska, and V.I. Klimov, J. Phys. Chem. B **107**, 13765 (2003).
[22] I. Kang and F.W. Wise, J. Opt. Soc. Am. B **14**, 1632 (1997).
[23] A.D. Andreev and A.A. Lipovskii, Phys. Rev. B **59**, 15 402 (1999).
[24] G.E. Tudury, M.V. Marquezini, L.G. Ferreira, L.C. Barbosa, and C.L. Cesar, Phys. Rev. B **62**, 7357 (2000).
[25] G. Allan, Y.M. Niquet, and C. Delerue, Appl. Phys. Lett. **77**, 639 (2000).
[26] Y.M. Niquet, C. Delerue, G. Allan, and M. Lannoo, Phys. Rev. B **62**, 5109 (2000).
[27] J.C. Slater and G.F. Koster, Phys. Rev. **94**, 1498 (1954).
[28] X. Gonze *et al.*, Comput. Mater. Sci. **25**, 478 (2002).
[29] We use Hartwigsen-Goedecker-Hutter pseudopotentials.
[30] S.E. Kohn, P.Y. Yu, Y. Petroff, Y.R. Shen, Y. Tsang, and M.L. Cohen, Phys. Rev. B **8**, 1477 (1973).
[31] G. Martinez, M. Schlüter, and M.L. Cohen, Phys. Rev. B **11**, 651 (1975).
[32] E.A. Albanesi, C.M.I. Okoye, C.O. Rodriguez, E.L. Peltzer y Blanca, and A.G. Petukhov, Phys. Rev. B **61**, 16 589 (2000).
[33] S.-H. Wei and A. Zunger, Phys. Rev. B **55**, 13 605 (1997).
[34] M. Lach-hab, D.A. Papaconstantopoulos, and M.J. Mehl, J. Phys. Chem. Solids **63**, 833 (2002).
[35] This is justified by the large dielectric constant of PbSe.
[36] W.A. Harrison, *Electronic Structure and the Properties of Solids, The Physics of the Chemical Bond* (Freeman, New York, 1980).
[37] M. Graf and P. Vogl, Phys. Rev. B **51**, 4940 (1995).
[38] A. Selloni, P. Marsella, and R. Del Sole, Phys. Rev. B **33**, 8885 (1986).
[39] One must note that the main contribution to the total polarization comes from interatomic terms, not intra-atomic ones.
[40] N. Suzuki, K. Sawai, and S. Adachi, J. Appl. Phys. **77**, 1249 (1995).
[41] M. Cardona and D.L. Greenaway, Phys. Rev. **133**, A1685 (1964).
[42] C. Delerue and M. Lannoo, *Nanostructures—Theory and Modelling* (Springer-Verlag, Berlin, 2004).
[43] This is confirmed by an analysis of the confined states by projection on the bulk states.
[44] A. Zunger and L.-W. Wang, Appl. Surf. Sci. **102**, 350 (1996).

[45] The joint density of states is given by Eq. (1) with the optical matrix element replaced by a constant.
[46] C. Delerue, G. Allan, and M. Lannoo, Phys. Rev. B **64**, 193402 (2001).
[47] M. Shim and P. Guyot-Sionnest, J. Chem. Phys. **111**, 6955 (1999).
[48] G. Allan, C. Delerue, and Y.M. Niquet, Phys. Rev. B **63**, 205301 (2001).
[49] C. Delerue, M. Lannoo, and G. Allan, Phys. Rev. B **68**, 115411 (2001).